

# Composite Microbolometers with Tellurium Detector Elements

Stuart M. Wentworth *Member, IEEE*, and Dean P. Neikirk, *Senior Member, IEEE*

**Abstract**—A composite microbolometer has been constructed for possible use as a broad band submillimeter radiation detector. Theory, fabrication, and measurement of these devices are discussed, and a finite element thermal model is introduced. Our devices utilize nichrome load elements which can be impedance-matched to a planar antenna. The load elements are thermally coupled to tellurium detectors. We achieved room temperature responsivities of 120 V/W, and noise equivalent powers (NEP) as low as  $6.7 \times 10^{-9}$  W/ $\sqrt{\text{Hz}}$ . Performance appears to be limited by 1/f noise in the Te detector.

## I. BACKGROUND

ONE TYPE of detector that has been used extensively in the far-infrared (FIR) portion of the spectrum (wavelengths between  $100 \mu\text{m}$  and 1 mm, also known as the submillimeter band) is the bolometer, which operates by changing resistance in response to a change in temperature. This temperature change results from radiation absorption. In order to efficiently absorb incident radiation the detector must be comparable in size to the wavelength  $\lambda$  of the radiation, and be impedance-matched to free space. Conventional bolometers are typically several wavelengths square, which may be up to several square millimeters for longer FIR radiation. One such conventional bolometer is a millimeter and submillimeter power meter developed by Rebeiz *et al.* [1]. For this  $1 \text{ cm}^2$ ,  $1000 \text{ \AA}$  thick bismuth bolometer biased at 1 V, a responsivity of 1 mV/W was obtained for a 100 Hz modulation frequency.

A drawback of these conventional-type bolometers is their large thermal mass, which reduces the speed at which they can respond to temperature changes. Also, the noise equivalent power (NEP), which should be as small as possible for sensitive operation, increases approximately as the square root of the bolometer area. To improve performance for FIR applications, the thermal detector must therefore be as small as possible, and have a resistance strongly dependent on temperature. One approach separates the radiation absorber from the temperature sensor.

Manuscript received August 16, 1990; revised March 13, 1991. This work was supported by the National Science Foundation under grant No. ECS-8552868.

S. M. Wentworth is with the Department of Electrical Engineering, Auburn University, 200 Broun Hall, Auburn, AL 36849-5201.

D. P. Neikirk is with the Department of Electrical Engineering, The University of Texas at Austin, Austin, TX 78712.

IEEE Log Number 9104774.

The absorbing material is chosen to efficiently capture the incoming radiation (and so must have an area of about  $\lambda^2$  and a sheet resistance equal to the free-space impedance), but can be relatively thin to give a low thermal mass. The temperature sensor material is chosen to produce very large changes in resistance with changing temperature, and must be in intimate thermal contact with the absorber, but may otherwise be very small and highly resistive. This composite structure can have an overall thermal mass which is much less than the conventional bolometer. A typical composite bolometer consists of Bi as the radiation absorber and gallium-doped germanium as the temperature sensor [2, 3]. This type of device has been used in astronomical applications [4].

The above treatment views the radiation in an optical framework, as a source of energy that is passively absorbed by a surface. Another view is to treat the radiation as an electromagnetic wave which is captured and guided by an antenna. Like the conventional bolometer, an antenna is comparable in size to the wavelength, but unlike the conventional bolometer, it dissipates no power. Instead, the antenna couples the power into a very small load resistor, which is then practically the only part of the system to change temperature. A small device like this also has a large thermal impedance which results in a relatively large change in temperature for a given amount of dissipated power. If the load resistor is the bolometer itself, extremely fast and sensitive performance can result. Such a detector is called a microbolometer [5], [6]. Antenna-coupled microbolometers have been shown to have higher responsivity, better sensitivity, and much faster response than conventional bolometers [7]. Since these are thermal detectors, they work well throughout the FIR spectral region without the capacitive roll-off associated with Schottky detectors.

The general frequency dependent responsivity equation for a bolometer is

$$r(\omega) = I_b Z_t(\omega) \frac{dR}{dT} \quad (1)$$

where  $r(\omega)$  is the responsivity in V/W,  $I_b$  is the current bias through the bolometer,  $dR/dT$  is the slope of resistance as a function of temperature, and  $Z_t(\omega)$  is the thermal impedance of the device, defined as the temperature rise in the bolometer per unit absorbed power. A large

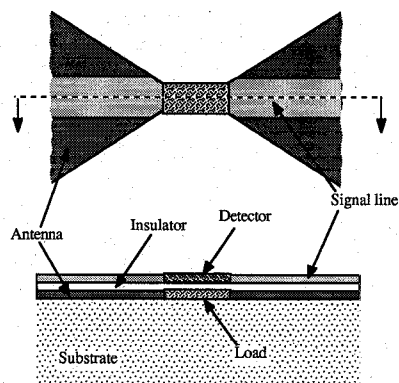


Fig. 1. Top view and cross section of a composite microbolometer. The load is impedance-matched to the bow-tie antenna, and is thermally coupled to a detector.

magnitude  $Z_l(\omega)$  is achieved by making the device small, as in a microbolometer. A small device can also change temperatures fast, so  $Z_l(\omega)$  can be large at modulation frequencies on the order of 20 kHz or more. Both the geometry and the material properties of the device will determine  $R$  and  $dR/dT$ , and will set limits on  $I_b$ .

A characteristic of a microbolometer detector is its linear relation between resistance and dissipated power. This property assumes that  $dR/dT$  is constant over the temperature range considered, and that the temperature change in the device is proportional to changes in its dissipated power. This leads to an expression for dc responsivity [6], (the response of a detector to a step change in dissipated power),

$$r_{dc} = I_b \frac{dR}{dW} \quad (2)$$

The dc curve of detector resistance  $R$  plotted as a function of dissipated power  $W$  therefore provides enough information to determine  $r$  and  $|Z_l|$  for the device.

Bismuth has been the material of choice for microbolometers in the past, primarily because its thin film resistivity is conducive to impedance-matching with planar antennas. Tellurium has been suggested as a bolometer candidate since thin film Te has a high value of  $dR/dT$  [8], and Te microbolometers have attained responsivities 100 times that of Bi microbolometers [9]. However, the resistance for the Te detector is too high to simply match with typical planar antenna impedances of 100–200  $\Omega$ .

One solution to the mismatched load problem is to design an antenna with a high impedance, as has been proposed by Rogers *et al.* using a twin slot antenna on a dielectric stack [10]. Another solution, which is the subject of this paper, is to separate the load from the detector in a composite microbolometer structure, as shown in Fig. 1. The load, which in this figure is impedance-matched to a bow-tie antenna, is in intimate thermal contact with, but is electrically isolated from, the detector element. Changes in load temperature will be quickly followed by changes in detector temperature, and hence by changes in detector resistance.

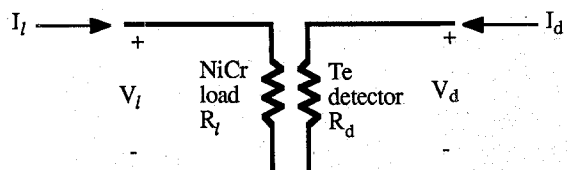


Fig. 2. A simple electrical circuit for the composite microbolometer.

## II. THEORY

The composite microbolometer can be represented by the simple electrical circuit shown in Fig. 2, where the load and detector elements are shown physically close together. For a given amount of power  $W_d$  dissipated in the detector, the dc responsivity  $r_d$  for the detector element by itself can be written:

$$r_d = \frac{dV_d}{dW_d} = \frac{V_d}{R_d} \frac{dR_d}{dW_d} \quad (3)$$

where  $V_d$ ,  $I_d$ , and  $R_d$  are the voltage, current, and resistance, respectively, associated with the detector. Equation (3) is the general equation for a conventional microbolometer. This equation can be modified to determine the composite microbolometer responsivity  $r_{CB}$ . The detector response to a change in power dissipated across the load element is

$$r_{CB} = \frac{dV_d}{dW_d} \frac{dW_d}{dW_l} = \frac{V_d}{R_d} \frac{dR_d}{dW_l} \quad (4)$$

where  $r_{CB}$  is the dc composite microbolometer responsivity, and the "l" subscripts denote load properties. In (4) there is an efficiency term relating how much heat is dissipated in the detector for a given amount of heat dissipated in the load:

$$\eta_{th} = \frac{dW_d}{dW_l} = \frac{r_{CB}}{r_d} \quad (5)$$

where  $\eta_{th}$  is the thermal coupling efficiency. This efficiency term depends on alignment of the top layer over the bottom layer, the separating insulator thickness, and the thermal properties of the separating layer. Since  $\eta_{th}$  is desired maximum, the separating insulator layer should be as thin as possible.

## III. FABRICATION

Composite microbolometers have been fabricated consisting of nichrome as the load, Te as the detector, and  $\text{SiO}_x$  as the insulator. These devices were fabricated on a glass slide substrate upon which gold contact pads had been electroplated. Gold was also used for both the antenna leads and the signal line. Both device layers were produced using a photoresist bridge technique [6]. In this procedure, applied to the load/antenna layer, the photoresist is patterned in such a way that a narrow photoresist bridge is left hanging at the apex of the bow-tie antenna. Metal for the antenna is then evaporated at normal incidence to the substrate, and the photoresist bridge casts



Fig. 3. SEM photograph of a photoresist bridge. The underlying NiCr load/antenna layer is slightly visible.

a shadow in the load region. The load material is then evaporated at an angle to the substrate such that deposition is accomplished under the photoresist bridge. A consequence of this approach is that load material also lies atop the antenna metal. This thin load layer is essentially shorted by the antenna metal and apparently does not effect antenna performance [6].

Vacuum deposition was carried out at less than  $10^{-6}$  torr, at deposition rates ranging from  $2 \text{ \AA/s}$  for NiCr to  $10 \text{ \AA/s}$  for Te and gold. The 80% Ni-20% Cr load was approximately  $1500 \text{ \AA}$  thick, in contact with a  $1500 \text{ \AA}$  thick gold bow-tie antenna. Following deposition of an  $1800 \text{ \AA}$  thick  $\text{SiO}_x$  layer (detailed below), the signal line/detector layer was fabricated using a second photoresist bridge process. An SEM photograph of a photoresist bridge used in fabrication of this layer is shown in Fig. 3. The load/antenna layer is barely visible. The Te detector was about  $1200 \text{ \AA}$  thick, contacted to a  $2000 \text{ \AA}$  thick gold signal line. The lengths and widths were about the same for both NiCr and Te elements, ranging from  $4.5$  to  $5.0 \mu\text{m}$ .

The  $\text{SiO}_x$  layer was formed by plasma-enhanced chemical vapor deposition. The CVD was carried out under a 170 torr pressure of  $\text{O}_2$  and 80 torr of silane. The  $\text{O}_2$  was passed through rf coils to produce an oxygen plasma, then mixed with silane just above the chip surface. The substrate was held at  $330^\circ\text{C}$ , and deposition took place over 40 minutes. To measure the thickness of the deposited oxide, a bare Si chip was placed next to the device chip during the CVD process. Thickness of the  $\text{SiO}_x$  layer on the bare Si chip was measured ellipsometrically. Contacts were opened through the  $\text{SiO}_x$  layer by a brief hydrofluoric acid etch. These contacts to the load/antenna layer were necessary for performing the speed of response measurement detailed in the next section.

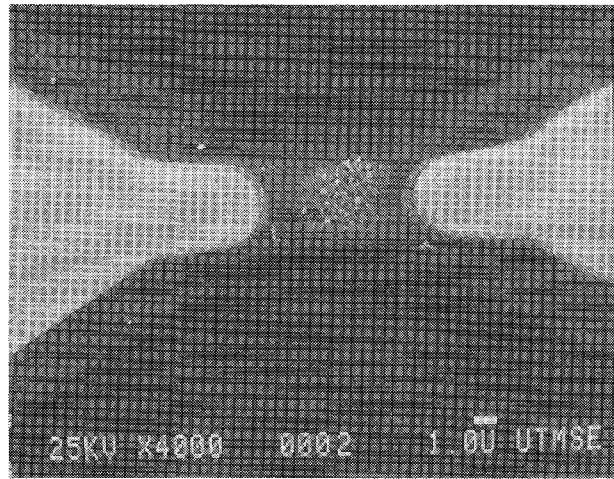


Fig. 4. SEM photograph of the composite microbolometer. The Te element is visible; the underlying NiCr load is not.

The composite microbolometer is shown in the SEM photograph of Fig. 4. Notice the grainy appearance of the Te element. The nichrome element is below the Te element and is therefore not visible in this photograph.

#### IV. MEASUREMENT

Performance of the composite microbolometer depends on responsivity of the Te detector. Since this is a bolometer detector, the Te resistance is a linear function of power dissipated in the Te element. Thus, the  $dR_d/dW_d$  in (3) can be found from the slope of the Te detector resistance-power plot of Fig. 5. For a  $0.75 \text{ V}$  bias, the Te detectors had a  $r_d$  of  $-510 \text{ V/W}$ .

The detector resistance  $R_d$  can also be measured as a function of power dissipated in the nichrome load element. Fig. 6 shows several such  $R_d - W_l$  plots at different Te detector bias voltages. Notice that the higher bias voltages result in lower resistance plots. The devices operate at a room temperature ambient, but the actual temperature in the vicinity of the Te element depends on its bias voltage, and on the heat transferred from the NiCr element. At higher  $V_d$ , the steady-state temperature of the Te element is higher. This results in lower overall resistance since thin film Te has a negative temperature coefficient of resistivity.

The dc responsivity  $r_{CB}$  of a composite microbolometer can be found by taking the slope of the resistance-power plot, just as was done for the conventional microbolometer (2). From Fig. 6, the slope  $dR_d/dW_l$  at  $V_{bd} = 0.75 \text{ V}$  leads to a responsivity  $r_{CB} = -120 \text{ V/W}$ . From this result and the result found for  $r_d$ , the thermal coupling efficiency is calculated as  $\eta_{th} = 0.24$ .

Fig. 7 illustrates the general scheme for measuring speed of response. Two 220 MHz RF sources are beat together at an adjustable frequency, and fed through a high pass filter to the antenna leads. The NiCr element changes temperature in response to the absorbed rf power, which is modulated at the beat frequency. This temperature change is felt by the Te detector. A bias network consist-

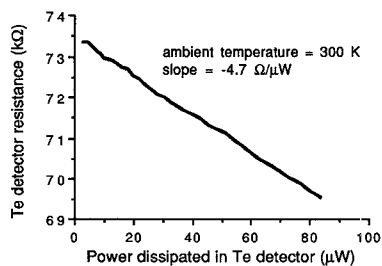


Fig. 5. The Te detector resistance is plotted as a function of power dissipated to determine dc responsivity of the free standing Te element.

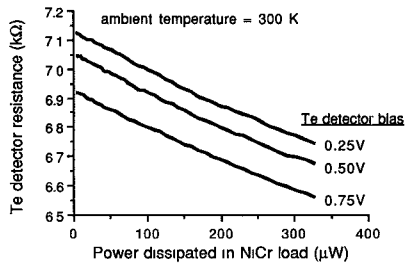


Fig. 6. Te resistance is plotted as a function of power dissipated by the nichrome load element. For a particular bias voltage  $V_{bd}$  across the Te detector, the slope of the plot can be used to calculate dc responsivity.

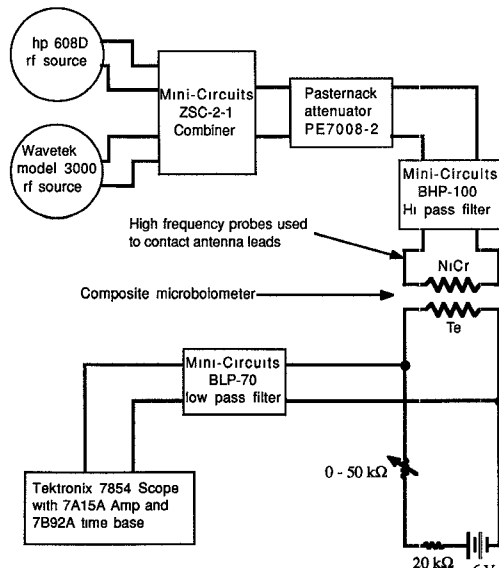


Fig. 7. RF measurement setup for the composite microbolometer.

ing of a 6 V battery and resistors supplies a steady bias across the Te detector. The signal drawn off the detector is fed through a low pass filter and monitored by an oscilloscope for beat frequencies ranging from 100 Hz to 200 kHz. The responsivity of the device is the ratio of this signal voltage to the power dissipated in the load element. This dissipated power is difficult to measure directly. However, at low frequencies the responsivity approaches the dc responsivity. Therefore, since dc responsivities have been determined, the power dissipated in the NiCr load element can be estimated. This dissipated power is assumed constant over the frequency range

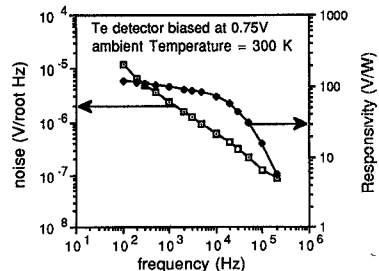


Fig. 8. Noise and responsivity are plotted as a function of beat frequency for a composite microbolometer with the Te detector element biased at 0.75 V.

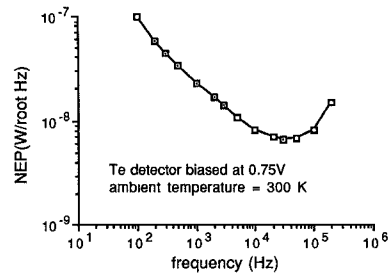


Fig. 9. Sensitivity for the composite microbolometer as a function of beat frequency, with the Te detector element biased at 0.75 V. Best performance occurs at about 30 kHz, where  $NEP = 6.7 \times 10^{-9} W/\sqrt{Hz}$ .

tested. The signal voltages are then divided by this dissipated power term to obtain responsivity as a function of frequency.

Fig. 8 shows the responsivity curve generated for the composite microbolometer at a Te detector bias of 0.75 V. A roll-off of responsivity begins at about 10<sup>4</sup> Hz, which is somewhat below where roll-off begins for a conventional microbolometer [6]. This is hardly surprising since the composite structure has a larger thermal mass to heat and cool. Fig. 8 also shows the noise voltage measured across the Te detector element at the same voltage. This noise is measured with a PAR 124A lock-in amplifier with 117 preamp over a bandwidth of 10% of the selected center frequency. Since the Johnson noise floor is about 10<sup>-8</sup> V/√Hz, it is clear that a 1/f-type noise is dominant. The NEP plot in Fig. 9 is calculated by dividing the noise by the responsivity. The device has a minimum NEP of 6.7 × 10<sup>-9</sup> W/√Hz at 30 kHz. For comparison, a Bi microbolometer typically has an  $r_{dc}$  of 20 V/W, and minimum NEP of 10<sup>-10</sup> W/√Hz at 10 kHz.

## V. THERMAL MODEL

A thermal model for the composite microbolometer is useful for better understanding of device operation, and for guiding design of an optimized structure. We consider the two dimensional cross section of the device, as shown in Fig. 10, and employ a finite difference approach where thermal resistance elements are used in a Gauss-Seidel iteration [11]. Effects in the y-direction will be neglected in this model. The device is broken up into a grid of rows and columns of elements. Since the problem is symmet-

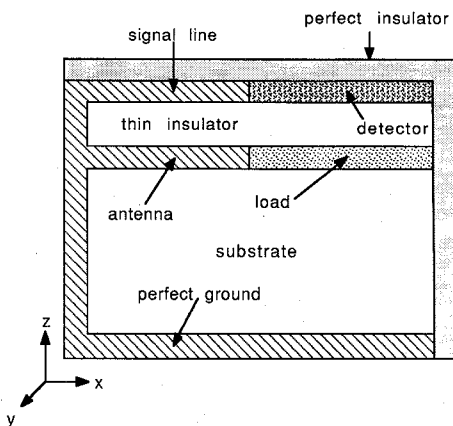


Fig. 10. Profile of half of the composite microbolometer, used for thermal modeling.

rical, the device is cut in half, and the cut surface is considered to be resting against a perfect insulator. To further simplify our model, we consider the antenna and signal lines to be perfect conductors, and the antenna/load and signal line/detector layers each occupy only one layer. The substrate and separating insulator layers are also assumed to have infinite electrical resistance.

The temperature at the center of each element is given by the Gauss-Seidel iterative equation

$$T_i = \frac{q_i + \sum_j \left( \frac{T_j}{Z_{ij}} \right)}{\sum_j \left( \frac{1}{Z_{ij}} \right)} \quad (6)$$

where  $T_i$  and  $T_j$  are the temperatures in the  $i$ th and  $j$ th element, respectively.  $Z_{ij}$  is the thermal resistance between the  $i$ th and  $j$ th element, and  $q_i$  is a heat generation term in an element. Our model must consider heat generation terms for both the NiCr load elements and the Te detector elements. For the detector elements

$$q_i = I_d^2 R_i \quad (7a)$$

and for the load elements

$$q_i = I_l^2 R_i \quad (7b)$$

$I_d$  and  $I_l$  are the currents through the elements, and  $R_i$  is the element resistance. For our NiCr load elements, the resistance is fairly constant with temperature. For the Te detector elements, the resistance depends on temperature by the equation

$$R_i = R_{io} + \frac{\Delta R_d}{\Delta T} \Delta T_o \quad (8)$$

where  $R_{io}$  is the ambient temperature,  $\Delta R_d/\Delta T$  is the detector temperature coefficient, and  $\Delta T_o$  is the temperature deviation from ambient.

Thus, for a given ambient temperature and a chosen bias current, the iterative procedure for steady-state is as follows:

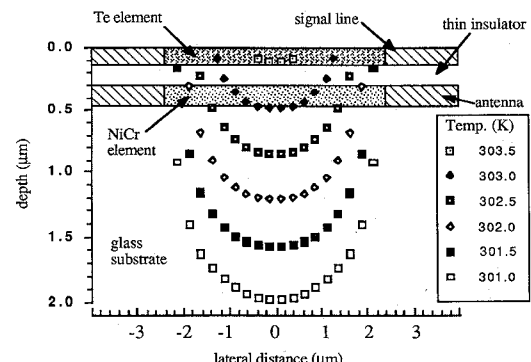


Fig. 11. Isotherms for the composite microbolometer with the following values for thermal ( $k$ ) and electrical ( $\sigma$ ) conductivities:

	Te	NiCr	SiO <sub>x</sub>	Glass
$k(\text{W/cm} \cdot \text{K})$	0.24	0.125	0.0013	0.014
$\sigma(\Omega \cdot \text{cm})^{-1}$	10.9	350	—	—

The figure is stretched in the depth direction relative to the lateral direction.

- 1) Determine thermal resistances in both the  $x$  and  $z$  directions for all elements. These are assumed constant for our degree of temperature change.
- 2) Determine electrical resistances for all detector elements in the  $x$ -direction at temperature  $T_i$  using (6). Initially, all elements are at ambient temperature.
- 3) Determine  $q_i$  from (7).
- 4) Use (8) to determine a new set of temperatures  $T_i$ .
- 5) Cycle through steps 2–4 until the changes in  $T_i$  are small.

This technique was used to generate the isothermal plot shown in Fig. 11. The material parameters in the thermal model may be adjusted to give dc responsivities which match both the composite microbolometer and the Te element by itself. These parameters are listed with the figure.

The thermal model predicts an improvement to  $r_{CB} = -158 \text{ V/W}$  ( $\eta_{th} = 0.36$ ) when the SiO<sub>x</sub> layer is thinned to 1000 Å. When a 1000 Å thick layer of diamond film is used, the thermal model predicts a drop in responsivity to about 12 V/W. The high thermal conductivity of the diamond film apparently acts as a thermal sink, preventing the high temperature gradients needed to produce a large responsivity. Thus, for a composite microbolometer, it is important to maximize the thermal conductance between the load and detector (i.e., the “vertical” direction), while minimizing it laterally. This is accomplished best by using an insulating material that is as thin as possible and has a reasonable thermal conductivity.

## VI. CONCLUSION

A composite microbolometer has been demonstrated which utilizes a NiCr load element thermally coupled to a Te detector. The sensitivity and speed of these devices have been measured, and the results have been used to formulate a thermal model for the composite structure. Although a conventional Bi microbolometer has a reasonable NEP, its low responsivity makes detection of low power levels difficult. The higher responsivity of our

composite structures may make it easier to detect these low levels, and could therefore ease amplification requirements in receiver systems. The thermal model predicts significant improvement in device sensitivity would result from a reduction of the separating insulator thickness. However, reducing  $1/f$  noise in the Te film offers perhaps the most potential for increased sensitivity.

The composite microbolometer technique opens the door for a variety of detector materials that might otherwise experience difficulty matching with a planar antenna. For instance, pyroelectric arrays have been used for infrared detection; an antenna-coupled composite microbolometer employing a pyroelectric detector such as lead zirconate titanate (PZT) could be an extremely sensitive detector of FIR radiation. This technique has also been suggested for use with superconductive detectors operating in the bolometric mode, where the resistance of the detector operating near the middle of the transition might be too low to match well to a planar antenna [12]. A composite transition-edge microbolometer (composite TREMBOL) would utilize the sharp  $dR/dT$  slope at the transition of a superconductor.

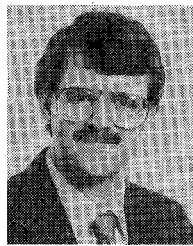
Finally, the emphasis in this paper has been on the composite microbolometer detector element, and not on the planar antenna. It is not known whether the signal line above the antenna metal (separated by the thin  $\text{SiO}_x$  layer) will have any significant effect on antenna performance.

#### ACKNOWLEDGMENT

The authors gratefully acknowledge A. Tsao's assistance with the SEM, and D. Miller's assistance with the dc testing.

#### REFERENCES

- [1] G. M. Rebeiz, C. C. Ling, and D. B. Rutledge, "Large area bolometers for millimeter-wave power calibration," *Int. J. Infrared and Millimeter Waves*, vol. 10, no. 8, pp. 931-936, 1989.
- [2] J. Clarke, G. I. Hoffer, and P. L. Richards, "Superconducting tunnel junction bolometers," *Rev. Phys. Appl.*, vol. 9, pp. 69-71, 1974.
- [3] N. S. Nishioka, P. L. Richards, and D. P. Woody, "Composite bolometers for submillimeter wavelengths," *Applied Optics*, vol. 17, no. 10, pp. 1562-1567, May 15, 1978.
- [4] M. W. Werner, J. H. Elias, D. Y. Gezari, M. G. Hauser, and W. E. Westbrook, "Observations of 1-millimeter continuum radiation from the DR 21 region," *Astrophys. J.*, vol. 199, pp. L185-L187, 1975.
- [5] T.-L. Hwang, S. E. Schwarz, and D. B. Rutledge, "Microbolometers for infrared detection," *Appl. Phys. Lett.*, vol. 34, no. 11, pp. 773-776, June 1979.
- [6] D. P. Neikirk, W. W. Lam, and D. B. Rutledge, "Far-infrared microbolometer detectors," *Int. J. Infrared and Millimeter Waves*, vol. 5, no. 3, pp. 245-278, Mar. 1984.
- [7] S. E. Schwarz and B. T. Ulrich, "Antenna-coupled infrared detectors," *J. Applied Phys.*, vol. 48, no. 5, pp. 1870-1873, May 1977.
- [8] B. H. Billings, W. L. Hyde, and E. E. Barr, "An Investigation of the Properties of Evaporated Metal Bolometers," *J. Opt. Soc. Am.*, vol. 37, pp. 123-132, 1947.
- [9] S. M. Wentworth and D. P. Neikirk, "Far infrared microbolometers made with tellurium and bismuth," *Electron. Lett.*, vol. 25, no. 23, pp. 1558-1560, Nov. 9, 1989.
- [10] S. M. Wentworth, R. L. Rogers, J. G. Heston, D. P. Neikirk, and T. Itoh, "Millimeter wave twin slot antennas on layered substrates," *Int. J. Infrared and Millimeter Waves*, vol. 11, no. 2, pp. 111-131, Feb. 1990.
- [11] J. P. Holman, *Heat Transfer*. New York: McGraw-Hill, 1981.
- [12] S. M. Wentworth and D. P. Neikirk, "A transition-edge microbolometer (TREMBOL) for far-infrared detection," in *Proc. SPIE: Superconductivity Applications for Infrared and Microwave Devices*, Orlando, Apr. 16-20, 1990.



**Stuart M. Wentworth** (S'88-M'90) was born in Pensacola, FL, in 1959. He received the B.S. degree in chemical engineering from Auburn University, Auburn, AL, in 1982, and the M.S. and Ph.D. degrees in electrical engineering from the University of Texas at Austin in 1987 and 1990, respectively.

From 1982 until 1985 he worked as a Quality Assurance Engineer for Dupont at Old Hickory, Tennessee. From 1986 until 1990 he was a Graduate Research Assistant for The University of Texas Microelectronics Research Center at Austin. He has modeled and tested tape-automated bonding (TAB) interconnects at high frequency, and has designed a TAB tape for use as a microwave interconnect. He has also investigated various antenna-coupled detectors for far-infrared radiation detection. He is currently an Assistant Professor in Electrical Engineering at Auburn University. His research interests include radiation detectors and monolithic microwave integrated circuits.

Dr. Wentworth is a member of the American Physical Society, and the American Society for Engineering Education.



**Dean P. Neikirk** (S'81-M'83-SM'89) was born in Oklahoma City, Oklahoma, on October 31, 1957. He received the B.S. degree in physics and mathematics from Oklahoma State University in 1979 and the M.S. and Ph.D. degrees in applied physics from the California Institute of Technology in 1981 and 1984, respectively.

He is currently an Associate Professor in Electrical and Computer Engineering at The University of Texas at Austin. He developed the first monolithic, high resolution focal plane detector array for use at wavelengths between 0.1 mm and 1 mm. In 1984 he received the Marconi International Fellowship Young Scientist Award for his work in this field. His current research interests concentrate on the use of advanced fabrication techniques, such as molecular beam epitaxy, for millimeter and submillimeter-wave device development. His work emphasizes novel structures for high frequency generation, detection, wave guiding, and radiation, suitable for monolithic integration.